Short communication

Ruthenium oxide-coated carbon felt electrode: A highly active anode for microbial fuel cell applications

Zhisheng Lv, Daohai Xie, Xianjun Yue, Chunhua Feng*, Chaohai Wei

The Key Lab of Pollution Control and Ecosystem Restoration in Industry Clusters, Ministry of Education, College of Environmental Science and Engineering, South China University of Technology, Guangzhou 510006, PR China

ARTICLE INFO

ABSTRACT

Enhancing the anode performance is a critical step for improving the power output of microbial fuel cells (MFCs). This study presents an active anode that involves the use of ruthenium oxide (RuO_2)-coated carbon felt electrode for MFC applications. Cathodic electrodeposition was performed to decorate the carbon felt surface with the RuO_2 films composed of submicron-/nano-sized particles. Increasing the amount of charge applied for the electrodeposition resulted in the increase in power performance of MFCs that were inoculated either with the pure culture or the mixed microbial consortia. The dual-chamber MFC equipped with the RuO_2-coated anode reached the maximum power density of $3.08\,W\,m^{-2}$ (normalized to the projected area of anode), increased by 17 times as compared to that obtained with the MFC with the bare anode. Cyclic voltammetry (CV) and electrochemical impedance spectra (EIS) results provided evidence that there was a substantial improvement in electron transfer between the microbes and the anode. The results demonstrate that RuO_2 interacts electrochemically with the cells and has ability to facilitate extracellular electron transfer.

1. Introduction

Microbial fuel cell (MFC) is a bioreactor capable of producing electricity by oxidizing organic compounds with the help of microorganisms. The low power output of MFCs compared to the well-developed chemical fuel cells (CFCs) represents the bottleneck in hurdling its practical application as a sustainable power source [1]. The efficiency in electron transfer from the bacteria to the anode of MFCs is thought to be an important factor limiting the anode performance and thereby the power output [2]. Many efforts were made to improve the electron transfer efficiency and thus the anode activity by modifying the commonly used carbon-based anode materials with (i) electroactive species such as quinones [3–5], Mn^{4+} [6], or neutral red [6,7] that exhibit fast and reversible redox behavior and function as an electron shuttle facilitating electron transfer, or (ii) highly conductive species such as conducting polymers [3,8], CNTs [9,10], metal particles [11,12] that are important for the improvement in the physical properties of the anode including electrical conductivity, specific surface area, and/or biocompatibility for microbial growth.

Ruthenium oxide (RuO_2) is recognized as an important material for a wide range of electrochemical applications including the use of RuO_2 as an excellent electrocatalyst for CO and methanol oxidation in fuel cells [13], and a promising electrode material used in supercapacitors [14,15]. Nano-sized RuO_2 particles are of particular interest for these applications owing to their fast and reversible redox behavior in a wide potential window, large surface area, high chemical stability and favorable metallic conductivity. These characteristics seem to be beneficial in terms of their application as the anode materials in MFCs. To date, however, no studies were conducted to examine the feasibility of using RuO_2 nanoparticles in the anode of MFCs; it is unclear whether RuO_2 is toxic to the cells or otherwise well suited to facilitate electron transfer between the cells and the anode.

This study presents the first report on evaluating power performance of a MFC equipped with the RuO_2-based anode. The anode was prepared by coating the carbon felt electrode with the RuO_2 films via electrodeposition. Although not feasible on a large scale, expensive materials including Ru and other metals (e.g., Au and Pt [11,12,16]) used in MFCs may provide useful insights into the reaction mechanisms, which should be quite understood before the MFC can be scaled up for practical applications. To investigate electron transfer between the bacteria and the anode, electrochemical studies including cyclic voltammetry (CV) and electrochemical impedance spectra (EIS) measurements were conducted.

* Corresponding author. Tel.: +86 20 39380502; fax: +86 20 39380588.
 E-mail address: chfeng@scut.edu.cn (C. Feng).

2. Materials and methods

2.1. Decoration of the carbon felt anode with RuO₂ via electrodeposition

The bare anode substrate was a piece of carbon felt (3.0 cm × 2.0 cm × 0.5 cm) which was connected with the external circuit by a Ti wire (0.8 mm in diameter) embedded inside it. Prior to electrodeposition, the carbon felt was cleaned in a hot H_2O_2 (10%, 90 °C) solution for 3 h, followed by thorough rinse with deionized water and dried at 60 °C. The electrodeposition of the RuO_2 films on the carbon felt was conducted from a $RuCl_3$ (0.05 M) solution at room temperature. The three-electrode electrochemical cell including a working electrode (carbon felt), a reference electrode (saturated calomel electrode, SCE) and a counter electrode (Pt mesh) was used for the cathodic electrodeposition. A constant current density of 5 mA cm⁻² (normalized to the projected area of anode) was applied to form the RuO_2 films. The total charge passed to the working electrode was varied in the range from 0 to 50 C cm⁻². The freshly prepared RuO_2-decorated carbon felt anode was then thoroughly rinsed with distilled water and air-dried at room temperature.

2.2. X-ray photoelectron spectroscope (XPS) tests

The XPS technique was used to analyze the elemental composition and oxidation state of the elements that exist on the modified carbon felt surface. XPS spectra were measured with an Axis Ultra DLD spectrometer (Kratos Analytical Ltd.) by employing AlKα ($h\nu$ = 1486.6 eV) irradiation as the photosource, with a primary voltage of 15 kV and an emission current 10 mA. The analysis chamber pressure during scans was 5×10^{-9} Torr.

2.3. MFC construction, operation and tests

The dual-chamber MFC consisting of the modified anode described above and a bare carbon felt cathode (3.0 cm × 2.0 cm × 0.5 cm) was constructed, separated by a cation exchange membrane (Zhejiang Qianqiu Group Co., Ltd., China). Each cell chamber made of polycarbonate has an effective volume of 25 mL. The anode chamber was inoculated with *Shewanella decolorationis* S12 which was grown on the lactate-growth medium including 10 mM lactate and 0.1 M phosphate buffer solution (PBS)-based nutrient solution (pH 8.0) consisting of 5.84 g L⁻¹ NaCl, 0.10 g L⁻¹ KCl, 0.25 g L⁻¹ NH₄Cl, 10 mL of vitamin solution and 10 mL of mineral solution. The cathode chamber was fed with a PBS solution (0.1 M, pH 7.0) containing 50 mM potassium hexacyanoferrate as the electron acceptor. MFC tests with mixed microbial consortia that originally inoculated with activated sludge collected from the Coking Wastewater Treatment Plant (Shaogang, China) were also performed. The inoculated MFCs were repeatedly fed with lactate as the electron donor and operated over one month.

For comparisons, a series of dual-chamber MFCs were constructed with modified anodes at different RuO_2 concentration that was controlled by varying the applied charge for the electrodeposition. All MFCs were operated at 30 °C. A 32-channel voltage collection instrument (AD8223, China) was used to record the cell voltages with a 500 Ω external resistance. The cell power density and polarization curves were obtained by varying the external resistor over the range from 4000 to 20 Ω when the performance of MFC approached steady state. The voltage at different resistances was recorded when its value had less than 2 mV-change in 1 min. Current density (I) was calculated as $I = V$ (cell voltage)$/R$ (external resistance), and power density (P) was calculated as $P = V \times I$. Both I and P were normalized to the projected area of anode surface.
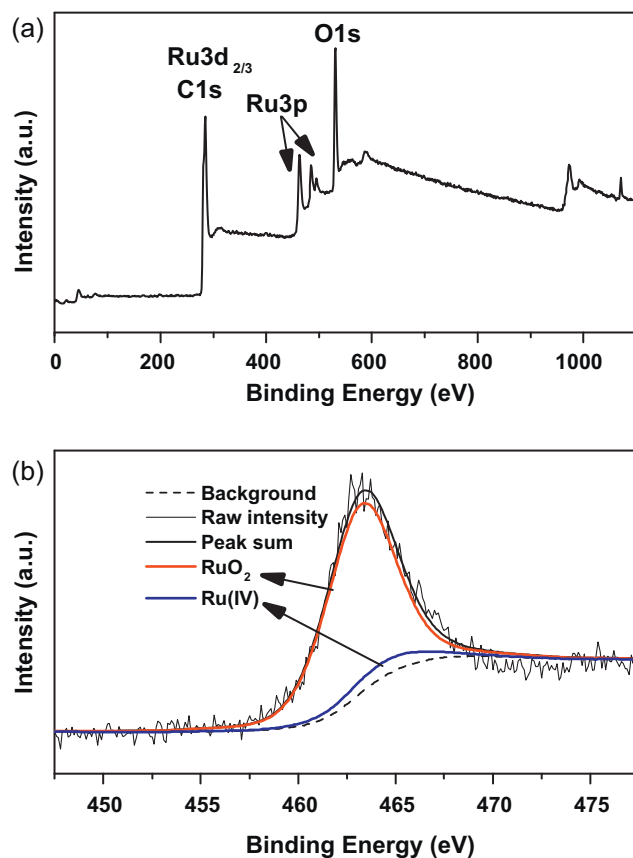

Fig. 1. The representative XPS (a) survey and (b) Ru 3p₃/₂ taken from the modified carbon felt surface. The amount of charge applied for the electrodeposition of RuO_2 was 50 C m⁻².

The CV and EIS measurements were performed using the anode as the working electrode, the cathode as the counter electrode, and a SCE inserted in the anode chamber as the reference electrode. The impedance spectra were recorded at the open circuit potential (OCP) and in the frequency range from 10,000 to 0.01 Hz with a sinusoidal excitation signal of 10 mV.

2.4. Scanning electron microscope (SEM) tests

The surface morphologies of the electrodes were examined using a Hitachi S-3000N SEM equipment. The stabilization of the bacteria attached to the anode was referred to the procedures described elsewhere [3]. Briefly, the sample (cut from the anode) was first immersed in 4% glutaraldehyde solution for 5 h. It was then rinsed with a PBS solution (pH 7.0) three times, followed by dehydration with increasing concentration of ethanol (34%, 50%, 75%, and 95%) for 10 min each and further rinses in isoamyl acetate twice (10 min each time). The sample was dried at CO₂-critical point for 3 h. Before SEM tests, the sample was sputtered with a thin coating layer of gold.

3. Results and discussion

3.1. XPS results

The wide-scan XPS survey spectrum (Fig. 1a) taken from the modified carbon felt surface reveals Ru 3p₁/₂ and Ru 3p₃/₂ at 486 and 464 eV in addition to C 1s and O 1s. Due to the overlapping of C 1s with Ru 3d₃/₂, the oxidation states of Ru species were determined by the XPS of core-level Ru 3p₃/₂ (Fig. 1b). By curve fitting, it was
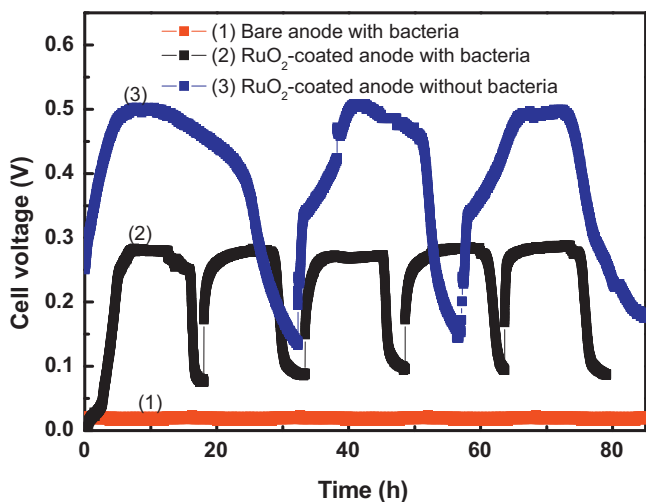
Fig. 2. Comparison of cell voltage output between the MFC equipped with the RuO$_2$-coated anode and that with the bare anode. The amount of charge applied for the electrodeposition of RuO$_2$ was 50 C m^{-2}. The external resistance was 500 Ω. The feed solution was fed with fresh lactate-growth medium including 20 mM lactate when the voltage dropped below 50 mV.

noted that the spectra could be decomposed into two peaks that were supposed to RuO$_2$ and Ru(IV) species with the binding energy equal to 463.2 and 464.4 eV, respectively [17]. The relative area under the peak curve of RuO$_2$ accounted for >90% of the total area, confirming RuO$_2$ is a major component that was introduced onto the carbon felt electrode via electrodeposition.

3.2. Performance of MFCs equipped with the RuO$_2$-coated carbon felt anode

Fig. 2 clearly shows that the RuO$_2$-coated carbon felt anode exhibited substantially better power performance than the bare anode. The typical voltage-generation profile [3] was observed for the RuO$_2$-coated anode (Fig. 2) when *S. decolorationis* was inoculated into the anode chamber, suggesting that RuO$_2$ is non-toxic to the bacteria. To further verify this point, toxicity tests in planktonic cultures were also performed in the presence and absence of RuO$_2$. The microbial growth of *S. decolorationis* S12 was examined by measuring the protein content as a function of time, according to the Bradford method [18]. It was found that the presence of RuO$_2$ did not alter the growth rate of *S. decolorationis* (data now shown).

The stable voltage produced by the carbon felt anode decorated with RuO$_2$ was found to be 1.8 times larger compared to the value relative to the bare anode. Comparison between two curves recorded with repeatable operations suggested that the Coulombic efficiency in the presence of RuO$_2$ was considerably higher, as evident from the larger voltage and the longer discharge time observed. No voltage output was achieved when the bacteria were absent from the anode chamber. It should be noted that under such a case the open circuit voltage (OCV) was approximately zero. These results suggest that the RuO$_2$-coated anode did not appreciably catalyze the electrochemical oxidation of lactate.

The tests of MFCs at different RuO$_2$ concentration were conducted in order to determine the effect of the applied charge for the electrodeposition on the power performance. Upon variation of the charge, changes in the overall power performance curves and the polarization curves were obtained (Fig. 3a). Despite the quite similar OCV observed, the voltage dropped more severely with the increasing current density when less amount of charge
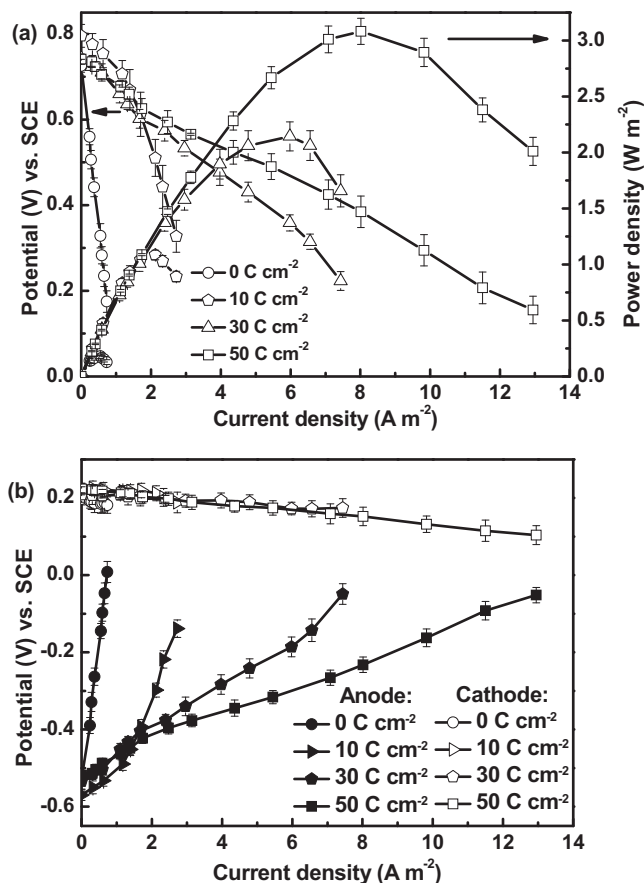

Fig. 3. (a) Power density curves and cell polarization curves, and (b) anode and cathode polarization curves of four MFCs inoculated with *S. decolorationis* S12 varying in anodes modified with different RuO$_2$ surface concentration. The applied charge density for the formation of RuO$_2$ contained in four anodes was 0, 10, 30 and 50 C cm^{-2}, respectively. The data point shown represents the average on triplicate measurements obtained from three independent experiments ± standard deviations.

was applied. The bare anode resulted in a limited current density of 0.73 A m^{-2}, which was 16.7 times less than 12.94 A m^{-2} obtained from the RuO$_2$-coated anode (50 C cm^{-2}). The maximum power density was found to be 0.18, 1.08, 2.14 and 3.08 W m^{-2}, in relation to the anodes with the applied charge of 0, 10, 30 and 50 C cm^{-2}, respectively. The RuO$_2$-coated anode (50 C cm^{-2}) exhibited an increase in power density by a factor of 17 as compared with the bare anode. These results clearly show that the increase in the amount of the electrodeposited RuO$_2$ resulted in the enhanced power performance. To the best of our knowledge, the maximum power density of 3.08 W m^{-2} (normalized to the projected area of anode) represents a high value reported for a dual-chamber MFC so far.

Anode and cathode polarization curves were performed in an attempt to identify the increased anode performance was mainly responsible for improving the overall power performance. As shown in Fig. 3b, the change in anode working potential as a function of increasing current density was highly dependent on the applied charge for the formation of RuO$_2$ films. In contrast, the impact of the applied charge on the variation in the cathode polarization curves was insignificant. For example, for the MFC with the bare anode, a significant rise in the anode potential from −0.53 to 0.01 V was observed by increasing current density from 0 to 0.73 A m^{-2}. However, for the MFC with the RuO$_2$-coated anode (50 C cm^{-2}), the increase in current density from 0 to 0.73 A m^{-2} only caused a small change in the anode potential (from −0.52 to −0.50 V). The smaller
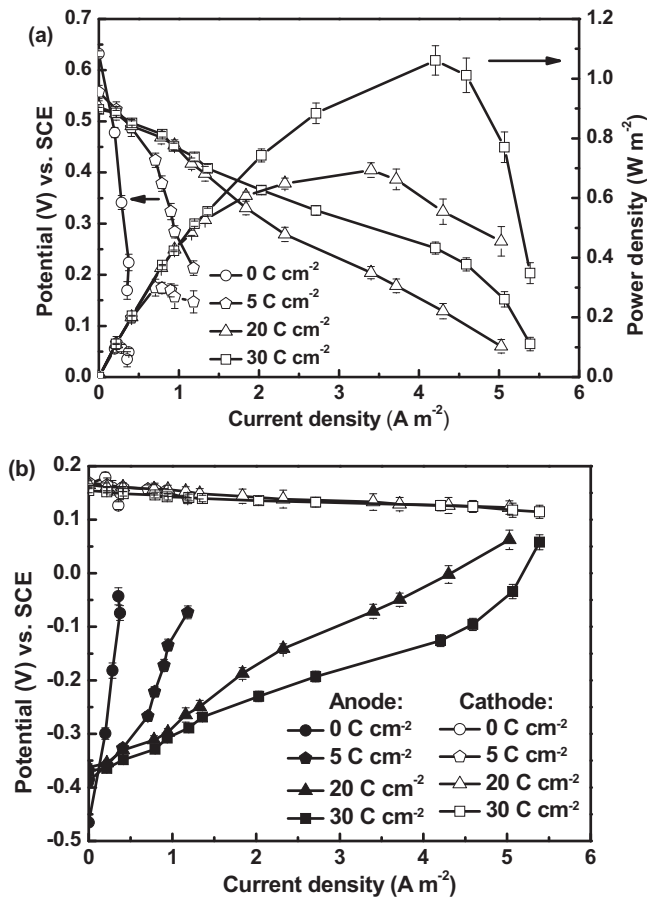
Fig. 4. (a) Power density curves and cell polarization curves, and (b) anode and cathode polarization curves of four MFCs inoculated with mixed microbial consortia varying in anodes modified with different RuO_2 surface concentration. The applied charge density for the formation of RuO_2 contained in four anodes was 0, 5, 20 and 30 C cm^{-2}, respectively. The data point shown represents the average on triplicate measurements obtained from three independent experiments ± standard deviations.

driving force (in the form of overpotential) required for the bio-electrochemical reactions at high currents indicates the role of RuO_2 in enhancing the bio-electroactivity of the anode system.

Performance evaluation of MFCs with the mixed microbial consortia further demonstrated that the RuO_2-coated anodes were capable of generating considerably higher power density than the bare anode (Fig. 4a). It was evident that the charge applied for the formation of RuO_2 coated on the anode positively affected the power and polarization performance, in direct analogy to what occurs for MFCs with the pure culture. For example, increasing the charge from 0 to 30 C cm^{-2} increased the power performance by a factor of 11 up to 1.06 W m^{-2}. Also, this effect turns out to be attributed to enhancement of anode performance other than cathode performance (Fig. 4b).

3.3. SEM results

The SEM results (Fig. 5) confirmed that the RuO_2 films were uniformly formed on the bare carbon felt surface upon electrodeposition. The electrodeposited RuO_2 films consisting of submicron-/nano-sized particles had a nanocomposite network structure, suggesting a substantial increase in the specific surface area of the anode. The SEM images shown in Fig. 5b and c were taken after inoculating the anode with the pure culture over 30 d; however, it was noticeable that no bacteria were attached on the RuO_2
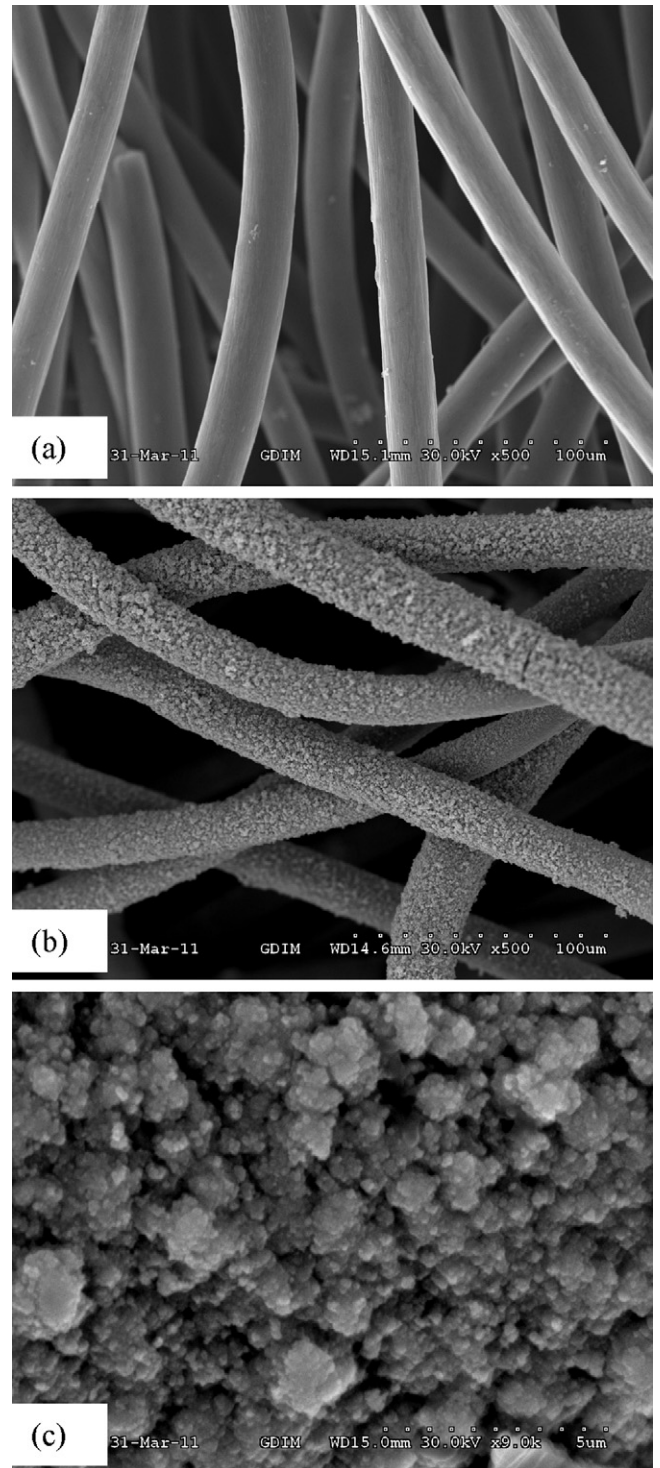

Fig. 5. SEM images of the (a) as-received carbon felt, and (b and c) RuO_2-coated carbon felt with different magnifications after the anode was inoculated over 30 d. The amount of charge applied for the electrodeposition of RuO_2 was 50 C m^{-2}.

surfaces. This finding is not consistent with previous observations that the incorporation of particles such as CNTs [9,10], Au [11,12] can accelerate biofilm formation. For these previous studies, bacteria available in the solid biofilm were believed to be useful for the transfer of electrons from the substrate to the anode. In contrast, for our study using the RuO_2-coated anode with *S. decolorationis*, planktonic cells that did not adhere on the electrode surface should be responsible for microbial current generation.
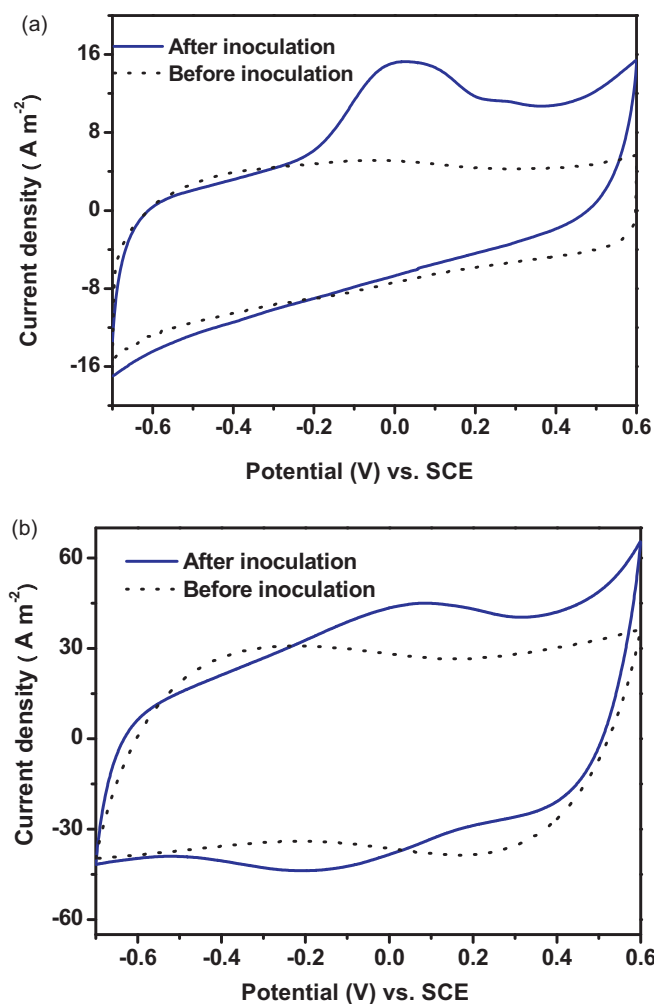
(a)

(b)

Fig. 6. CVs of (a) the bare anode and (b) the RuO$_2$-coated anode recorded before and after inoculation in a substrate-depleted medium (0.1 M PBS, pH 8.0). The scan rate was 10 mV s^{-1}. The amount of charge applied for the electrodeposition of RuO$_2$ was 50 C m^{-2}.

3.4. CV and EIS results

Fig. 6a and b shows CVs obtained for the bare and RuO$_2$-coated anodes before and after inoculation with the pure culture. An oxidation peak at +0.05 V (vs. SCE) was distinct from the CV curve taken on the bare anode in a substrate-depleted medium, but a reduction peak was not evident, indicating that a completely irreversible redox reaction occurred. In contrast, an anodic peak at +0.10 V (vs. SCE) and a cathodic peak at −0.20 V (vs. SCE) were clearly visible in the CV curve of the RuO$_2$-coated anode. These quasi-reversible voltammetric peaks should be relative with redox-active flavins, which are secreted from *Shewanella* and play a role in mediating extracellular electron transfer [19]. The quasi-reversible feature of this redox couple was indicative of fast electron transfer process. It can also be seen from Fig. 6a and b that the redox currents associated with redox-active flavins produced on the RuO$_2$-coated anode were at least 3 times larger than those in relation to the bare anode. This was resulted from the improvement in the specific surface area as illustrated by the SEM images. The significant increase in the currents reflects that more amounts of redox mediators are involved for electron transfer, thus accounting for the improvement in the anode electron transfer efficiency and the power performance.

Fig. 7 shows the EIS data (in the form of Nyquist plots) of bare and RuO$_2$-coated carbon felt anodes, which were obtained after the
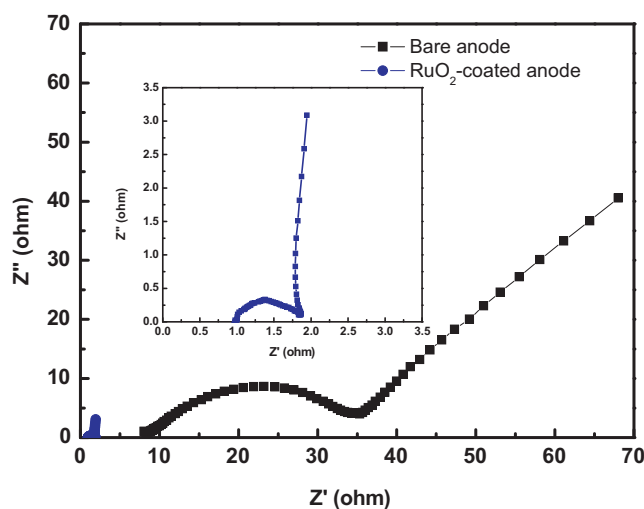

Fig. 7. EIS data of the bare and RuO$_2$-coated anodes after the MFCs were operated over 60 h. The amount of charge applied for the electrodeposition of RuO$_2$ was 50 C m^{-2}.

MFCs were operated over 60 h in the presence of the pure culture. The high frequency intercept with the *x*-axis in the Nyquist plots is associated with the ohmic resistance in the anode. It was noticeable that the anode ohmic resistance for the RuO$_2$-coated anode was significantly lower than that for the bare anode. Moreover, the significant decrease in the magnitude of the Nyquist arc suggested a decrease in the electron transfer resistance. These results demonstrate that the RuO$_2$-coated carbon felt anode is able to decrease the anode ohmic resistance and facilitate the kinetics of the bioelectrochemical reactions.

Here, it is proposed that the active electron transfer in the RuO$_2$-coated anode is possibly attributed to the increased specific surface area as well as the fast and reversible redox reactions between the oxidation states Ru (IV) and Ru (II) in a wide potential range. It is well known that RuO$_2$ is an active electrode material for supercapacitor applications [14,15]. For the case of using RuO$_2$ as the MFC anode material, electrons liberated from microbial oxidation of lactate are stored by RuO$_2$, when electron transfer is hindered by the immediate unavailability of electron acceptor (e.g., hexacyanoferrate in this study). The ability to store electrons thus contributes to temporarily maintain active electron transfer between the cells and the anode. Once a new source of electron acceptor is available, the electrons stored can be immediately released and transferred to the terminal electron acceptor.

4. Conclusions

This was the first finding that RuO$_2$ represents a favorable anode material of MFCs. Incorporation of RuO$_2$ submicron-/nanosized particles on the carbon felt anode increased the maximum power density to 3.08 W m^{-2}, which was 17 times higher than that obtained with the bare anode. The high specific surface area, the low resistance and the capacitive behavior of the RuO$_2$-coated anode are considered to be responsible for the active anode electron transfer process. Further studies are conducted in our group to evaluate how the capacitance of the anode material quantitatively affect the anode electron transfer and thereby the power performance.

References

[1] A. Rinaldi, B. Mecheri, V. Garavaglia, S. Licoccia, P.D. Nardo, E. Traversa, Energy Environ. Sci. 1 (2008) 417–429.
[2] U. Schröder, Phys. Chem. Chem. Phys. 9 (2007) 2619–2629.
[3] C. Feng, L. Ma, F. Li, H. Mai, X. Lang, S. Fan, Biosens. Bioelectron. 25 (2010) 1516–1520.
[4] C. Feng, F. Li, H. Liu, X. Lang, S. Fan, Electrochim. Acta 55 (2010) 2048–2054.
[5] M. Adachi, T. Shmomura, M. Komatsu, H. Yakuwa, A. Miya, Chem. Commun. 7 (2008) 2055–2057.
[6] D.H. Park, J.G. Zeikus, Appl. Microbiol. Biotechnol. 59 (2002) 58–61.
[7] K. Wang, Y. Liu, S. Chen, J. Power Sources 196 (2011) 164–168.
[8] J. Niessen, U. Schröder, M. Rosenbaum, F. Scholz, Electrochem. Commun. 6 (2004) 571–575.
[9] L. Peng, S. You, J. Wang, Biosens. Bioelectron. 25 (2010) 1248–1251.
[10] X. Xie, L. Hu, M. Pasta, G.F. Wells, D. Kong, C.S. Criddle, Y. Cui, Nano Lett. 11 (2011) 291–296.
[11] M. Sun, F. Zhang, Z. Tong, G. Sheng, Y. Chen, Y. Zhao, Y. Chen, S. Zhou, G. Liu, Y. Tao, H. Yu, Biosens. Bioelectron. 26 (2010) 338–343.
[12] Y. Fan, S. Xu, R. Schaller, J. Jiao, F. Chaplen, H. Liu, Biosens. Bioelectron. 26 (2011) 1908–1912.
[13] W. Sugimoto, T. Saida, Y. Takasu, Electrochem. Commun. 8 (2006) 411–415.
[14] M. Peckerar, Z. Dilli, M. Dornajafi, N. Goldsman, Y. Ngu, R.B. Proctor, B.J. Krupsaw, D.A. Lowy, Energy Environ. Sci. 4 (2011) 1807–1812.
[15] J.W. Long, K.E. Swider, C.I. Merzbacher, D.R. Rolison, Langmuir 15 (1999) 780–785.
[16] H. Park, D. Sanchez, S.K. Cho, M. Yun, Environ. Sci. Technol. 42 (2008) 6243–6249.
[17] Y. Chen, X. Zhang, D.C. Zhang, Y.W. Ma, J. Alloys Compd. 511 (2012) 251–256.
[18] M.M. Bradford, Anal. Biochem. 72 (1976) 248–254.
[19] E. Marsili, D.B. Baron, I.D. Shikhare, D. Coursolle, J.A. Gralnick, D.R. Bond, PNAS 105 (2008) 3968–3973.